Article

Generalized Predictive Control Scheme for a Wind Turbine System

Fahimeh Shiravani [1,*] , **Jose Antonio Cortajarena** [1,*] , **Patxi Alkorta** [1] **and Oscar Barambones** [2]

1 Engineering School of Gipuzkoa, University of the Basque Country, Otaola Hirib. 29, 20600 Eibar, Spain; patxi.alkorta@ehu.eus
2 Engineering School of Vitoria, University of the Basque Country, Nieves Cano 12, 01006 Vitoria, Spain; oscar.barambones@ehu.eus
* Correspondences: fahimeh.shiravani@ehu.eus (F.S.); josean.cortajarena@ehu.eus (J.A.C.)

Abstract: In this paper, a generalized predictive control scheme for wind energy conversion systems that consists of a wind turbine and a doubly-fed induction generator is proposed. The design is created by using the maximum power point tracking theory to maximize the extracted wind power, even when the turbine is uncertain or the wind speed varies abruptly. The suggested controller guarantees compliance with current constraints by applying them in the regulator's conceptual design process to assure that the rotor windings are not damaged due to the over-current. This GPC speed control solves the optimization problem based on the truncated Newton minimization method. Finally, simulation results, which are obtained through the Matlab/Simulink software, show the effectiveness of the proposed speed regulator compared to the widely used Proportional-integral controller for DFIG.

Keywords: wind energy; wind turbine; DFIG (doubly-fed induction generator); MPPT (maximum power point tracking); GPC (generalized predictive control)

1. Introduction

Increased use of renewable energy sources, such as sunlight and wind, especially in developing countries, helps to reduce greenhouse gas emissions while meeting energy demands. In general, wind energy has lower environmental costs than many other sources of energy. Wind turbines can help reduce total air pollution and carbon dioxide emissions [1].

Due to their properties, double fed induction generators (DFIG) are the most commonly employed generators in wind energy conversion systems. The main benefit of DFIG in wind turbine plants is that they can keep the amplitude and frequency of the output voltages constant regardless of the speed of wind blowing on the blade. As a result, DFIG may be directly linked to the AC power supply and stay synchronized with it continuously. Other benefits include the ability to control the power factor (e.g., keeping it at unity) while requiring minimal maintenance of the wind turbine power electronics components [2].

The developed controller must push the turbine's rotor speed to the optimum point to maximize the generated power. However, wind speed fluctuates rapidly over time, and since wind turbine systems are inherently non-linear, this is a procedure that introduces several uncertainties [3]. As a result, in variable-speed wind turbine plants, DFIG regulation is essential to ensure high efficiency and cost-effectiveness. The proportional-integral (PI) regulator is one of the most commonly used control approaches in DFIG control schemes due to its simplicity and universality. Nevertheless, its parameter performance can be influenced by uncertainties and nonlinearities.

Various advanced control systems for obtaining the maximum power from the wind have been developed to overcome this challenge. Control systems such as: sliding mode control [4,5], adaptive method [6], fuzzy logic control [7–9], H-infinity approach [10], and model predictive control (MPC) [11,12].

Due to its structural benefits, such as minimal sensitivity to parameter variations, rejection of external disturbances, and quick dynamic reactions, MPC is acknowledged as one of the most resilient control systems among the techniques mentioned [13,14], and has been employed to regulate DFIG in different aspects, such as: active and reactive power control [15–17], current control [18–20], and torque control [21,22].

Generalized Predictive Control (GPC) is an innovative attempt to unify distinct principles of predictive control. It generates a series of control signals to optimize the regulated system's control effort, within each sample interval [23]. GPC is one of the most popular model based predictive controllers, as a result of its accomplishments in SISo and MIMO industrial system regulation. Some authors have taken advantage of the properties of this type of predictive controller to regulate DFIG. For instance, in [24,25], GPC is employed to regulate the rotor currents of DFIG and in [26] a pitch controller based on GPC has been proposed.

In this paper, an efficient speed control scheme based on GPC is designed which aims to maximize the extracted wind power even when the turbine is uncertain or the wind speed varies abruptly. After being combined with two PI and SVPWM current controllers, the GPC controller is cascaded to the PI-SVPWM scheme. The inner loop's fast dynamics and low total harmonic distortion (THD) are achieved by carefully adjusting the stator currents' PI regulators and employing SVPWM's seven-vector symmetrical modulation. As a result, the predictive controller references are responded to very rapidly by this loop. Consequently, a cascaded GPC-PI controller is built that has remarkable fast dynamics, high precision, high robustness, low THD, and a medium computational cost.

The following items are the major contributions of this work:

- Modulating the current of the rotor-side converter (RSC), using the GPC speed regulator in order to track the optimal wind turbine speed by applying Maximum Power Point Tracking (MPPT);
- Truncated Newton (TNC) optimizer is incorporated into the controller design process [27]. TNC uses a truncated Newton algorithm to minimize the rotor current to the bounds;
- Highlighting the out-performance of the proposed method compared to the existing techniques by using Matlab/Simulink.

This paper is organized as follows: in Section 2 the GPC has been applied to the mechanical speed of DFIG. The effectiveness of the proposed controller is obtained by numerical simulations, and they are presented in Section 3. Finally, the conclusion has been discussed in Section 4.

2. GPC Design for Mechanical Speed of DFIG

The major components of the DFIG wind conversion system include a wind turbine and a DFIG. The shaft of the wind turbine is mechanically linked to the shaft of the generator through a gearbox. The stator of the DFIG and the grid side converter (GSC) will be connected to the grid after the synchronisation process. The rotor of the generator is connected to the grid through the rotor side converter (RSC) and the GSC in a back to back configuration. Both converters are modulated by using the SVPWM technique. The overall diagram of DFIG wind turbine system is presented in Figure 1.
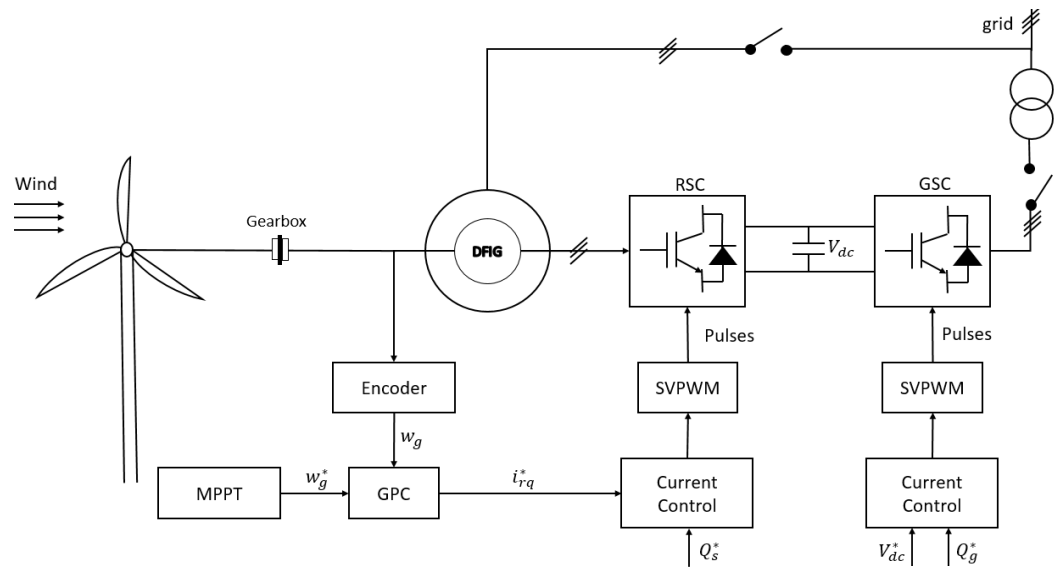
Figure 1. The overall block diagram of DFIG wind turbine system.

2.1. Turbine Model

Wind turbines absorb kinetic energy of the wind by using blades. Wind creates pressure on the blades, which causes the blades to spin. The blades are attached to a driving shaft that spins an electric generator, which provides power. The extracted power mainly depends on wind speed, air density, and blade radius and it is calculated as [28]:

$$P_m(\beta, \lambda, v) = \frac{1}{2} C_p(\lambda, \beta) \rho \pi R^2 v^3 \tag{1}$$

where ρ denotes the air density, R is the radius of the area that is covered by the blades, v stands for wind speed, C_p is power coefficient of wind turbine and it is measured by the manufacturer at several wind speeds. C_p depends on pitch angle of the blade (β) and the tip-speed ratio (λ), which is defined as:

$$\lambda = \frac{R w_t}{v} \tag{2}$$

where w_t is the turbine speed. Based on Equation (2), it is apparent that if the turbine or rotor speed is kept constant, any change in wind speed causes the tip-speed ratio to change, resulting in a change in the power coefficient C_p, as well as the generated power from the wind turbine. If, on the other hand, the rotor speed is regulated in response to changes in wind speed, the tip-speed ratio may be kept at an optimal point, potentially resulting in the system's maximum power generation. By considering Equations (1) and (2), it is obtained:

$$P_m(w) = k_{w_t} w_t^3 \tag{3}$$

where,

$$k_{w_t} = \frac{1}{2} C_p(\lambda, \beta) \rho \pi \frac{R^5}{\lambda^3} \tag{4}$$

The main components of a wind energy conversion system are an aeroturbine that converts wind energy into mechanical energy, a gearbox that increases speed while decreasing torque, and a generator that converts mechanical energy into electrical energy. The wind turbine's rotor spins at the speed w_t, driven by the input wind torque T_t. The generator receives the turbine torque in its shaft through the gearbox ($\frac{T_t}{\eta}$), and produces an electromagnetic torque T_e at the w_g generator velocity. The mechanical model of the system is depicted as follows [29]:

$$J_t \dot{w}_t + B_t w_t = T_t - T_e \eta \tag{5}$$

$$J_g \dot{w}_g + B_g w_g = \frac{T_t}{\eta} - T_e \tag{6}$$

$$T_t w_t = T_e w_g \tag{7}$$

$$w_g P = w_r \tag{8}$$

where J_t and J_g are the moment of inertia of turbine and generator, respectively. B_t and B_g stand for viscous friction coefficient of the turbine and generator. Additionally, P stands for the number of pair of poles of the machine and w_r is the electrical rotor speed. The relation between the turbine angular velocity and generator rotor rotational speed shows the gear ratio as follows:

$$\eta = \frac{w_g}{w_t} \tag{9}$$

Finally, considering Equations (5)–(9), the mechanical model on the generator side might be compressed as follows:

$$J\dot{w}_g + B_v w_g = T_t/\eta - T_e \tag{10}$$

which $J = J_t/\eta^2 + J_g$ and $B_v = B_t/\eta^2 + B_g$. Mechanical torque is obtained as:

$$T_t(w_t, \lambda, \beta) = k_{w_t} w_t^2 \tag{11}$$

Moreover, the C_p coefficient of the turbine which is used in this work is represented as:

$$C_P(\lambda, \beta) = c_1 \left(\frac{c_2}{\lambda_i} - c_3 \beta - c_4 \right) e^{\frac{-c_5}{\lambda_i}} + c_6 \lambda \tag{12}$$

$$\frac{1}{\lambda_i} = \frac{1}{\lambda + 0.08} - \frac{0.035}{\beta^3 + 1} \tag{13}$$

DFIG wind turbine is developed to perform in a variety of wind speeds while optimizing energy harvest. In this regard, it exists an optimum λ_{opt} that maximise power coefficient C_p^{max} and consequently the extracted power when the pitch angle $\beta = 0$. Then, from Equations (2) and (9), the generator optimal speed reference is obtained as:

$$w_g^* = \frac{\lambda_{opt} \eta v}{R} \tag{14}$$

2.2. DFIG Model

As it is well known, field-oriented control (FOC) theory has been applied to simplify the DFIG equations in the past few decades. The stator currents of the DFIG are represented as a vector of d and q components in this approach. The d component represents the magnetic flux, whereas the q component represents the generator's torque. Therefore, by using the rotatory reference frame, the stator flux linkage vector (Ψ_s) is aligned with d axis which means $\Psi_s = \psi_{sd}$ and $\psi_{sq} = 0$. Thus, considering FOC method the DFIG model is obtained as:

$$i_{sd} = \frac{|\Psi_s|}{L_s} - \frac{L_m}{L_s} i_{rd} \tag{15}$$

$$i_{sq} = -\frac{L_m i_{rq}}{L_s} \tag{16}$$

$$T_e = -\frac{3P}{2} \frac{L_m}{L_s} \Psi_s i_{rq} \tag{17}$$

$$P_s = \frac{w_e}{P} T_e \tag{18}$$

$$Q_s = \frac{3}{2} v_{sq} \left[\frac{v_{sq}}{w_e L_s} - \frac{L_m}{L_s} i_{rd} \right] \tag{19}$$

$$\Psi_s = \frac{v_{sq}}{w_e} \tag{20}$$

$$v_{rd} = R_r i_{rd} + \sigma L_r \frac{di_{rd}}{dt} - (w_e - w_r)\sigma L_r i_{rq} \tag{21}$$

$$v_{rq} = R_r i_{rq} + \sigma L_r \frac{di_{rq}}{dt} + (w_e - w_r)(\sigma L_r i_{rd} + \frac{L_m}{L_s}\Psi_s) \tag{22}$$

where L_s and L_r are inductances of stator and rotor, respectively, and L_m is the mutual inductance. w_e is the synchronous velocity of the rotor and σ is the coefficient of magnetic dispersion which is obtained as $\sigma = 1 - \frac{L_m^2}{L_s L_r}$.

The electromagnetic torque equation is achieved as:

$$T_e = K_T i_{rq} \tag{23}$$

where K_T is the torque constant, and it is defined as:

$$K_T = -\frac{3P}{2}\frac{L_m}{L_s}\Psi_s \tag{24}$$

2.3. Research Gap

The wind conversion system is often regulated with a vector control technique with cascading PI-current and power loops. According to the nonlinear dynamics and uncertainties expected in these systems, to increase the performance of the system, a more robust controller should be used. For this purpose, a model-based regulator, such as GPC, can be a good candidate. The capacity of these control systems to systematically address restrictions and achieve effective performance has had a considerable impact on control engineering practice [30].

2.4. GPC Design

Regarding the model, assuming that the DFIG rotor electrical time constant is much faster than the mechanical time constant, the dynamics associated with the DFIG rotor current controller blocks, the PWM modules, and the RSC and GSC blocks can be neglected. Therefore, the first order transfer function of the DFIG is simplified as:

$$\frac{w_g(s)}{i_{rq}^*(s)} = \frac{K_T/B_v}{(1 + s\tau_m)} \tag{25}$$

where $\tau_m = \frac{J}{B_v}$ is the mechanical time constant.

The design of the speed controller by using the GPC method will take place in discrete time since the GPC is of the discrete type. Hence, by using the first order transfer function of the DFIG, which is obtained in Equation (25) and applying the zero order holding discretization method, is achieved:

$$\frac{w_g(z^{-1})}{i_{rq}^*(z^{-1})} = \frac{B(z^{-1})}{A(z^{-1})} = \frac{b_0}{1 - az^{-1}} \tag{26}$$

In Equation (26), by considering $w_g(t)$ and i_{rq}^* as output and input of the system and replacing them with $y(t)$ and $u(t)$, respectively, it is feasible to obtain the following equation by combining the GPC theory and CARIMA model [31],

$$A(z^{-1})y(k) = B(z^{-1})z^{-d}u(k-1) + C(z^{-1})\frac{e(t)}{\Delta} \tag{27}$$

where $e(t)$ is uncorrelated (white) noise with zero mean, $\Delta = 1 - z^{-1}$ is the integrator, d is the dead time of the system, $B(z^{-1})/A(z^{-1})$ is the transfer function of the system,

and $C(z^{-1})$ can be treated as a filter that can be used to design disturbance rejection and noise reduction which its value may be set as 1 for simplicity.

The optimization problem in GPC algorithm finds the best control law which is obtained by minimizing the cost function [31],

$$J_c = \sum_{j=N_1}^{N_2} \delta(j)[\hat{y}(k+j|k) - w(k+j)]^2 \\ + \sum_{j=1}^{N_u} \gamma(j)[\Delta u(k+j-1)]^2 \tag{28}$$

where N_1 and N_2 are the minimum and maximum costing horizons, respectively. N_u is the control horizon, δ and γ are the control weights, $\omega(k+j)$ is a future reference sequence, $\Delta u(k)$ is the incremental control action, and $\hat{y}(k+j|k)$ is the optimum j step ahead prediction of the system output $y(t)$ on data up to time t. The objective of GPC is to estimate the future control sequence $u(k), u(k+1), \ldots$, such that the future plant output $y(k+1)$ is driven close to $\omega(k+1)$.

The optimal prediction of the future output expression is,

$$y = Gu + f \tag{29}$$

where G is the dynamic matrix and f is the free response term. Additionally, y, w, and u are defined as:
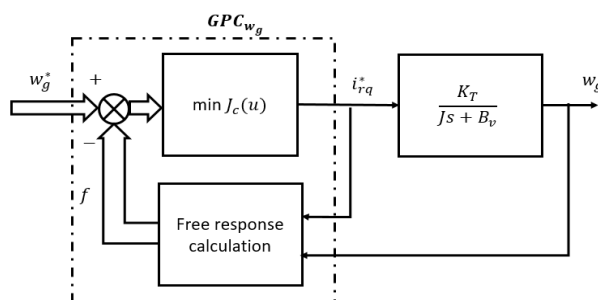
$$y = \begin{bmatrix} \hat{y}(k+d+1|k) \\ . \\ . \\ . \\ \hat{y}(k+d+N|k) \end{bmatrix}, w = \begin{bmatrix} w(k+N_1) \\ . \\ . \\ . \\ w(k+N_2) \end{bmatrix} \text{ and } u = \begin{bmatrix} \Delta u(k) \\ \vdots \\ \Delta u(k+N-1) \end{bmatrix}.$$

Finally, the vectors for the DFIG are described as follows:

$$w = w_g^* = \begin{bmatrix} w_g^*(k+N_1) \\ . \\ . \\ . \\ w_g^*(k+N_2) \end{bmatrix}, u = \begin{bmatrix} \Delta i_{rq}^*(k) \\ \vdots \\ \Delta i_{rq}^*(k+N-1) \end{bmatrix} \tag{30}$$

Remark 1. *The stability analysis of the GPC with $N_u = 1$ is provided in [32].*

The final control scheme of the controller is shown in Figure 2.

Figure 2. Block diagram of proposed control system.

2.5. Constraints on Rotor Windings

The ability to include control signal restrictions into the conceptual design phase is one of the key advantages of predictive controllers. Hence, in this study, the system limitations are situated in the control signal i_{rq}^*, which has a direct effect on the value of the three phase rotor currents of DFIG. As a result, the control signal i_{rq}^* must be constrained to an

upper and a lower limitation in the speed control design process by employing the TNC optimization method. Considering

$$\Delta i_{rq}^*(k) = i_{rq}^*(k) - i_{rq}^*(k-1) \tag{31}$$

then the bounds of $i_{rq}^*(t)$ which is associated to the electromagnetic torque, in the constraint form is expressed as:

$$\Delta I_{rq_{min}} \leqslant \Delta i_{rq}^* \leqslant \Delta I_{rq_{max}} \tag{32}$$

where,

$$\begin{aligned} \Delta I_{rq_{max}} &= I_{rq_{max}} - i_{rq}^*(k-1) \\ \Delta I_{rq_{min}} &= I_{rq_{min}} - i_{rq}^*(k-1) \end{aligned} \tag{33}$$

and in this scenario can be chosen as,

$$I_{rq_{max}} = -I_{rq_{min}} \tag{34}$$

3. Simulation Validation

This section outlines the effectiveness of the new GPC control strategy for wind turbine velocity control. This control technique intends to maximize energy conversion from the wind and, as a result, increase power generation by applying MPPT method. To achieve this, the wind turbine is required to track the variations in wind velocity in order to maintain the optimal tip speed ratio. The simulations are implemented using the software Matlab and Simulink, and the *SimPowerSystems* package is employed to obtain the prototypes for the wind turbine and the 7.5 kW generator. The specifications of the employed DFIG and turbine are listed in Tables 1 and 2, respectively.

Table 1. Rated parameters of the DFIG.

Parameters	Rated Value
Stator Voltage	380 V
Rotor voltage	190 V
Rated stator current	18 A
Rated rotor current	24 A
Rated speed	1447 rpm@50 Hz
Rated power	7.5 kW@50 Hz
Rated torque	50 Nm
Stator resistance	0.42 Ω
Rotor resistance	0.14 Ω
Magnetizing inductance	0.063 H
Stator leakage inductance	0.0018 H
Rotor leakage inductance	0.0023 H
Inertia moment	0.07 Kg·m^2
Viscous friction coefficient	0.0136 N·m·s

Table 2. Turbine parameters.

Parameters	Rated Value
λ_{opt}	3.6
R	2.25 m
ρ	1.22 kg/m^3
c_1, c_2, c_3, c_4, c_5 and c_6	15.9, 16, 0.02, 5, 21 and 9.12 $\times$ 10^{-3}, respectively
Inertia moment	5 kg·m^2
Viscous friction coefficient	0.001 N·m·s
Gearbox relation	8.2

As it has been explained, the generated power by a wind turbine is a function of tip speed ratio, pitch angle, and wind velocity. Considering Equation (14), the idea is to keep λ at its maximum value and let the turbine speed be based on the blowing wind speed. Maximizing λ results in maximum power coefficient and consequently, based on Equation (1), maximization of extracted power. Figure 3 shows the $C_p - w_t$ features for different wind speeds while pitch angle is zero. It can be observed that for different velocities of wind a unified maximum power factor can be obtained while the generator is working at different speeds. The optimal *lambda* according to the curves of Figure 3 corresponds to $\lambda_{opt} = 3.6$.
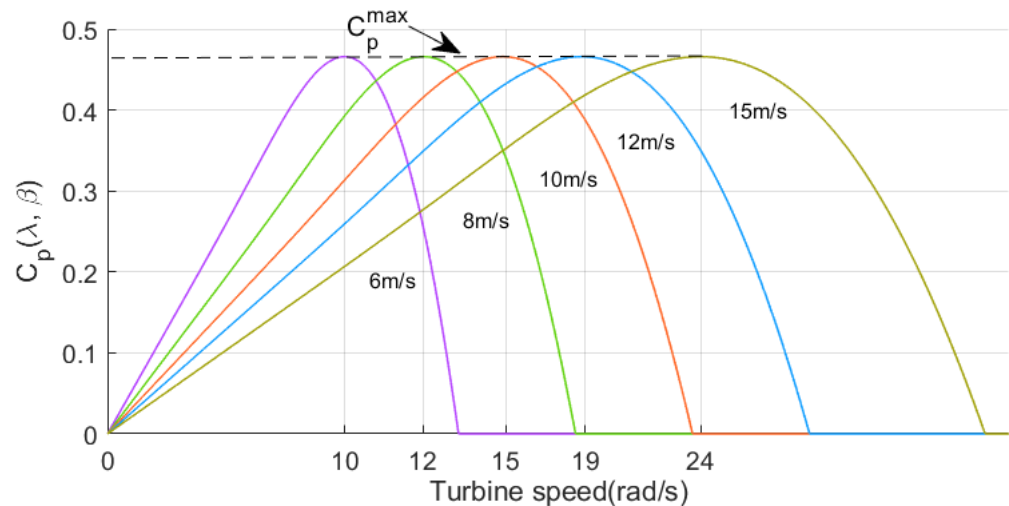
Figure 3. Power coefficient versus turbine speed for varying wind speeds.

In this proposal, a GPC method is being integrated into the speed loop to guarantee the optimum generated power. The number of the coefficients of the controller depends on the prediction horizon N. Although having a higher value for the prediction horizon enhances the control performance of the system, there will be a higher computational burden. Therefore, based on this compromise, the prediction horizon is set as $N = 5$, and considering that $d = 0$ as $N_1 = 1 + d$ and $N_2 = N + d$, it will be obtained $N_1 = 1$ and $N_2 = 5$. Additionally, the control horizon is taken as $N_u = 1$. The sampling time for all regulators is set as 100 µs. In this control scheme, the γ and δ parameters have to be tuned. The most optimal way is to keep the tracking weighting factor δ to unity and adjust γ. It is worth mentioning that for a smaller weighting factor, γ, the response time of the system is faster. In the following tests, γ is adjusted at 0.014.

As shown in Figure 4, for various wind speeds, there exists a generator speed in which the extracted power is maximum (MPPT).

Additionally, in the proposed controller the constraints on the rotor windings are integrated with the conceptual controller process, which implies that the linear solution is not valid to minimize the cost function [31]. Hence, in this work, the TNC optimization method is employed to minimize the cost function. The TNC function is written in the Simulink S-builder function by using the C programming language [27]. Furthermore, in the implementation of TNC, the maximum number of iterations that are used to solve the numerical solution can be specified. Due to this matter, there can be a compromise between the computational cost and the performance as well. In the provided tests, the number of iterations is set at 50.

In the presented work, two PI controllers are used to regulate the components of the rotor current i_{rd} and i_{rq}. The proportional and integral gains are adjusted to regulate the system as fast as possible by employing the frequency domain method [33]. Taking into consideration that the space vector pulse width modulation technique is implemented to operate at the switching frequency of 10 kHz, the established bandwidth for the PI

controllers is 1 kHz with a phase margin of 90°. In this regard, the obtained proportional and integral gains are $k_{pi} = 0.05$ and $K_{ii} = 5$.
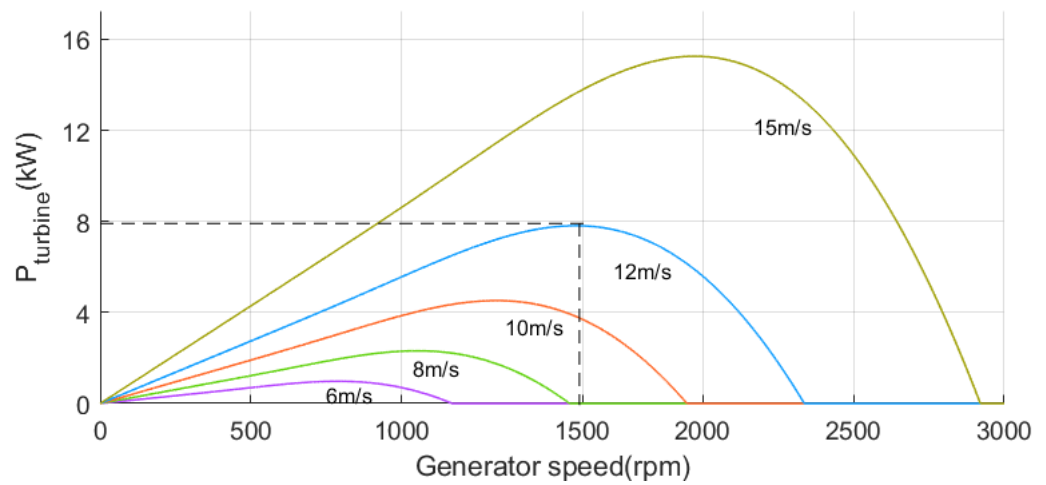

Figure 4. Turbine power-generator speed.

In general, the proposed GPC solves an optimization problem based on TNC at each sampling time, which is not linear. This technique is compared with a PI speed control technique in Figure 5. The PI speed control parameters are adjusted as $K_p = 14$ and $K_i = 90$, in order to obtain a fast response. It is supposed that wind is blowing at three different speeds, 7 m/s, 13 m/s, and 15 m/s.
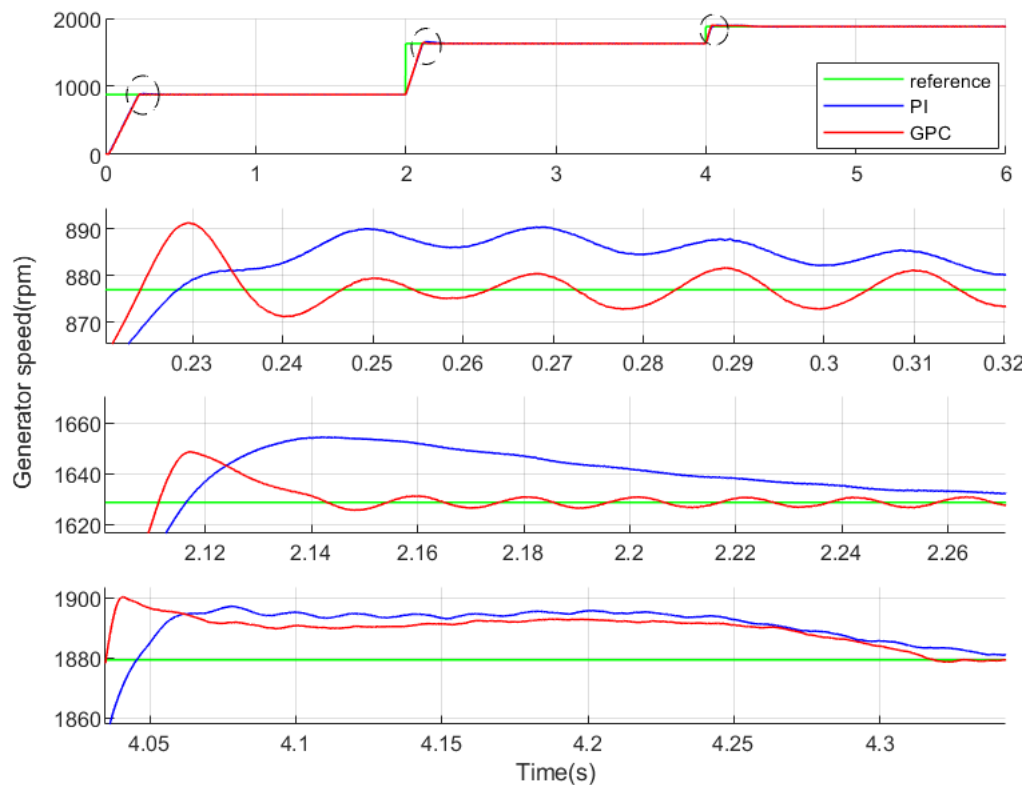

Figure 5. Comparison of the rotor speed of the DFIG, using PI and GPC methods.

In Figure 5, the DFIG speed performance by using the MPPT method and applying PI and GPC regulation methods is shown and highlighted. It can be seen that the GPC has better tracking performance than the PI controller. Additionally, by using GPC, the reach

time is shorter, and the convergence of the reference and real-speed signal is faster. This is happening thanks to the anticipatory nature of the GPC regulator as it is highlighted in the figure. This controller, by measuring the variations in the wind speed, starts to apply the changes some time ahead and can catch the modifications in wind speed faster than conventional controllers.

In Figure 6, the turbine torque at the DFIG shaft (T_t/η) and the DFIG electromagnetic torque (T_e) are shown at three different speeds. When stationary the values of both torques are equal, but during the transition periods the electromagnetic torque changes the sign in order to accelerate the machine as fast as possible based on Equation (6).
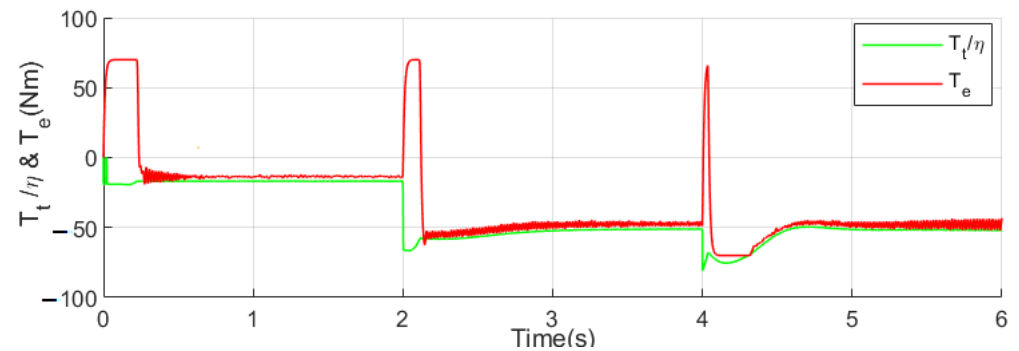
Figure 6. Turbine load torque and DFIG electromagnetic torque on the generator side.

Figure 7 shows the successful regulation of rotor current components i_{rd} and i_{rq}. Clearly, the value of i_{rd} is kept at 16.5 A and i_{rq} is bounded to its maximum value of 24 A. The reference of the i_{rq} is the output of the GPC speed regulator and, as it was explained before, the constraint of rotor current is applied in the conceptual GPC design process. Therefore, by obtaining good tracking performance of rotor current components, it is concluded that the proposed GPC-PI control scheme is successful in meeting the control objectives.
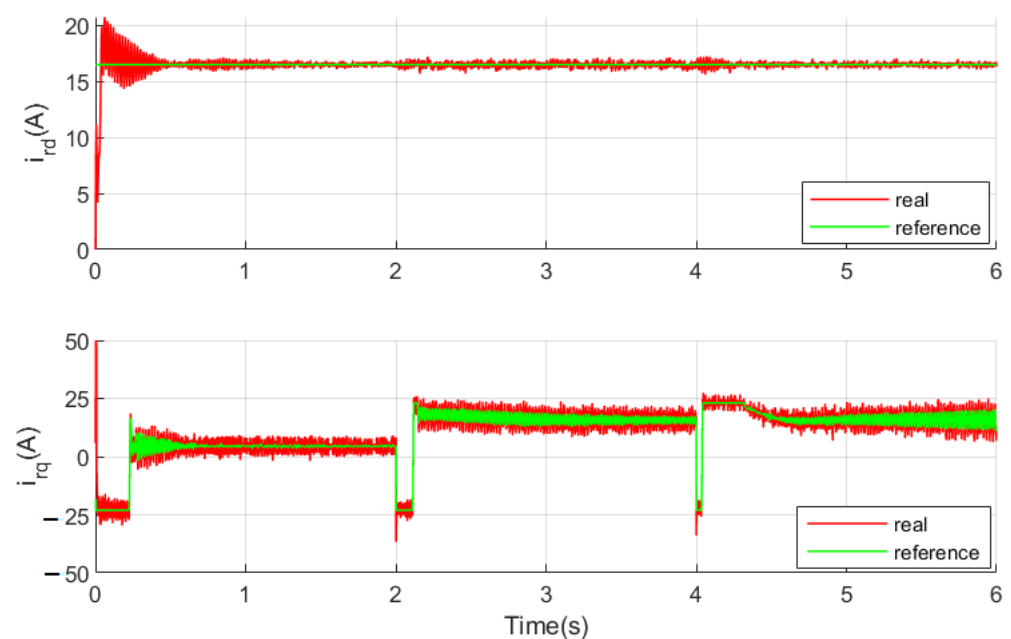
Figure 7. Rotor current components i_{rd} and i_{rq}.

The performance of the proposed method of power generation is depicted in Figure 8. The power that is generated by the turbine, the power that the stator delivers to the grid, the rotor power through converters, and, finally, the total power are plotted in this figure.

When the wind speed is 7 m/s DFIG is working sub-synchronous which means the rotor is absorbing energy from the grid through the converters (negative power). However, when wind speed is higher than 11.4 m/s the DFIG operation is over-synchronous, thus, the rotor power is positive since it is sent to the grid.
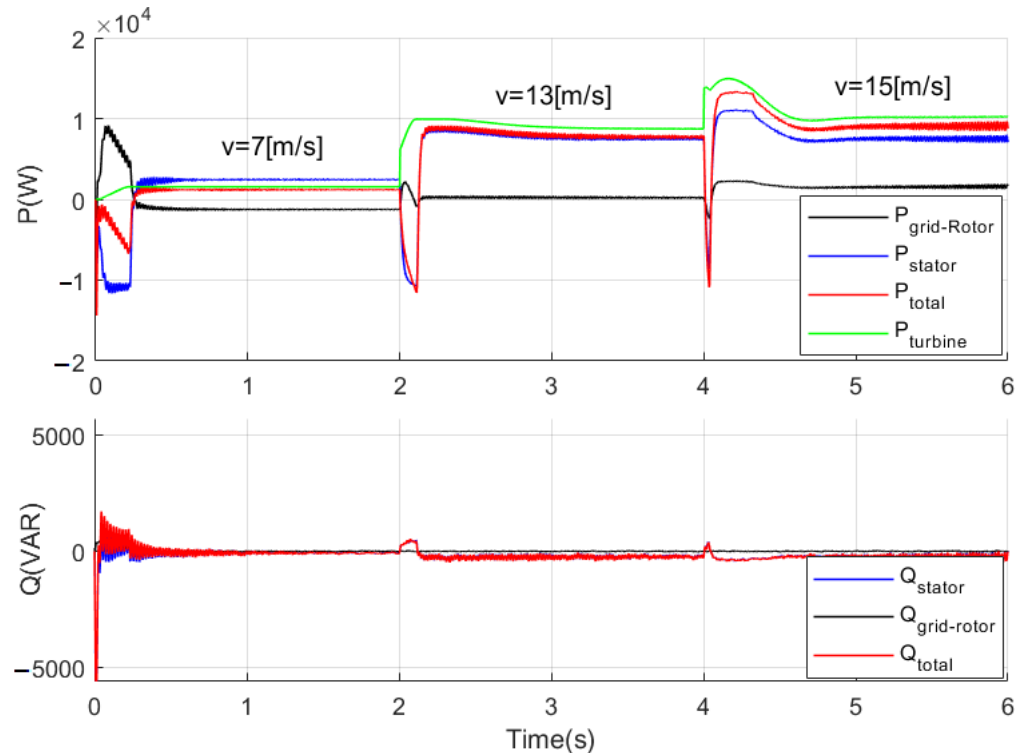
Figure 8. Active and reactive power for different wind speeds.

The rated power of the applied DFIG is 7.5 kW and that is the reason when stator power exceeds its nominal value, the pitch control is activated. This point is highlighted in Figure 9. Additionally, the C_p graph shows the success of the proposed control method in keeping the power coefficient factor at its optimum value when the pitch angle is zero. In addition, the value of the C_p is reduced as soon as the pitch angle starts to increase, in order to limit the maximum stator power to 7.5 kW as it is shown in the figure for wind speeds of 13 m/s and 15 m/s.

Figure 10 depicts the stator and rotor currents, respectively. As it is highlighted, the quality of the injected current to the grid is good. Moreover, as shown in the graph, as the generator speed varies, the frequency of the rotor current and its amplitude vary. The amplitude of the rotor current is coherent with the rotor modules d and q components, which imposed by the GPC-PI scheme controllers.

In Figure 11, a realistic wind speed profile is considered to show the success of the proposed method under real wind profile conditions. As it can be seen, the GPC speed regulator successfully controls the turbine in order to follow the reference according to the upcoming wind speed.
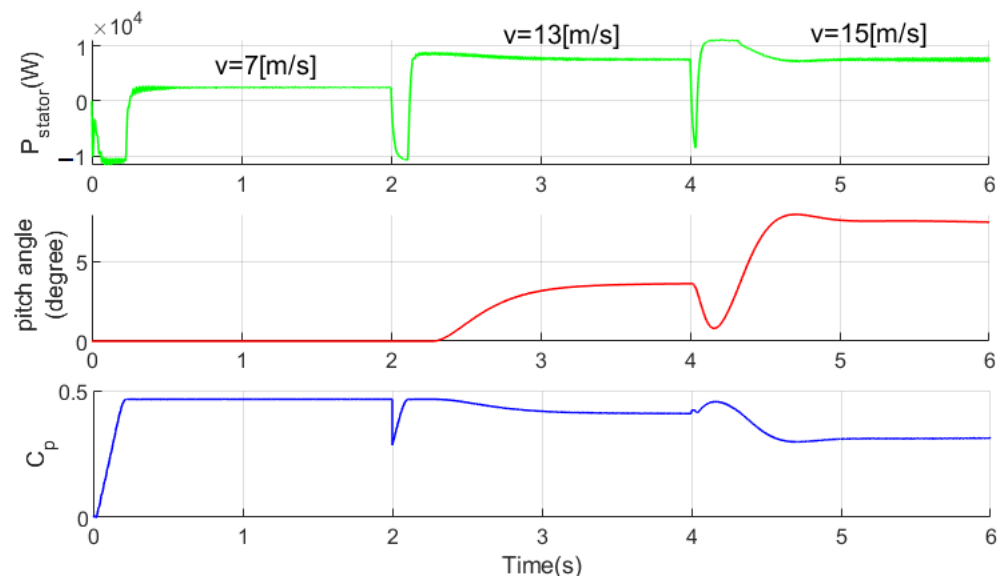
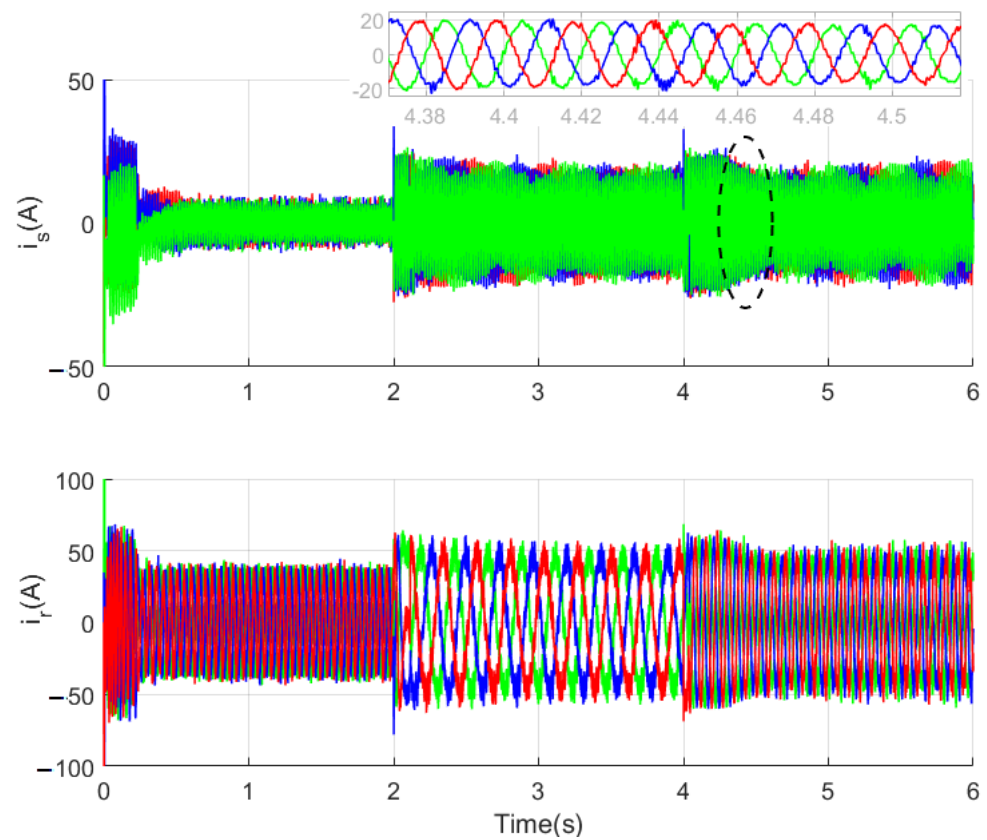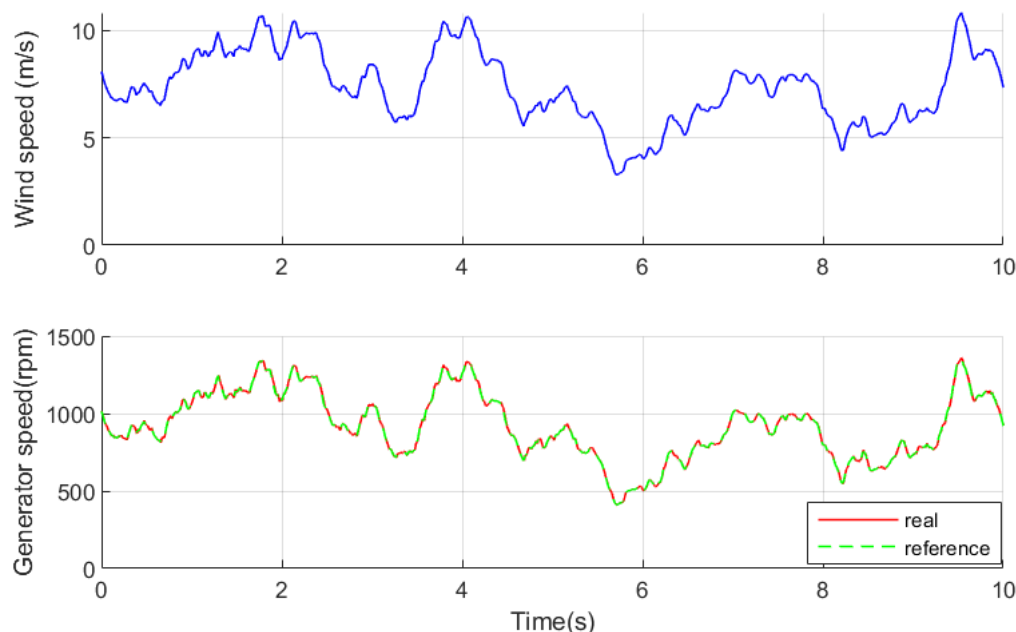**Figure 9.** Stator power, pitch angle, and C_p coefficient.

Figure 10. Stator and rotor three phase currents.

Figure 11. A realistic wind speed profile and the generator speed performance.

4. Conclusions

In this paper, a speed GPC scheme for the wind energy conversion systems is presented. The main objective is to control the turbine following the MPPT algorithm. For this purpose, the power coefficient is kept at its optimum value and the turbine's speed is adjusted by using GPC regulator responding to the upcoming wind velocity. Thus, the established control mechanism enables the wind turbine to operate at maximum power efficiency within a range of wind speeds. The constraint on the rotor windings are integrated into the GPC through the TNC optimizer in the conceptual control design process. The simulation results validate that the proposed regulator has a better performance compared to the exiting methods in controlling the variable speed wind turbine. For instance, in different ranges of wind speed the settling time of the DFIG velocity by using the proposed GPC controller is between 30 ms and 110 ms faster than the case that PI controller is employed.

Author Contributions: Conceptualization, F.S., J.A.C. and P.A.; methodology, F.S. and J.A.C.; software, F.S., J.A.C. and P.A.; validation, F.S., J.A.C. and P.A.; formal analysis, O.B.; investigation, F.S. and J.A.C.; resources, O.B.; data curation, J.A.C. and P.A.; writing–original draft preparation, F.S.; writing–review and editing, F.S., J.A.C., P.A. and O.B.; visualization, P.A. and O.B.; supervision, J.A.C. All authors have read and agreed to the published version of the manuscript.

Conflicts of Interest: The authors declare no conflict of interest.

References

1. Wind Energy Technologies Office. Wind Energy and the Environment. 2020. Available online: https://www.eia.gov/energyexplained/wind/wind-energy-and-the-environment.php (accessed on 17 December 2021).
2. Sample, C. Principles of Doubly-Fed Induction Generators (Dfig); Festo Didactic Ltee/Ltd. May 2011 Canada. Available online: https://citeseerx.ist.psu.edu/viewdoc/download?doi=10.1.1.726.2750&rep=rep1&type=pdf (accessed on 24 May 2022).
3. Barambones, O.; Cortajarena, J.A.; Calvo, I.; de Durana, J.M.G.; Alkorta, P.; Karami-Mollaee, A. Real time observer and control scheme for a Wind Turbine System based on a high order sliding modes. *J. Frankl. Inst.* **2021**, *358*, 5795–5819. [CrossRef]
4. Alzain, O.B.; Liu, X.; Kong, X. Optimized Sliding Mode Regulation based on PSO Algorithm for Nonlinear DFIG-WT. *J. Control Eng. Appl. Inform.* **2021**, *23*, 33–45.
5. Benbouhenni, H.; Bizon, N.; Colak, I.; Thounthong, P.; Takorabet, N. Simplified Super Twisting Sliding Mode Approaches of the Double-Powered Induction Generator-Based Multi-Rotor Wind Turbine System. *Sustainability* **2022**, *14*, 5014. [CrossRef]
6. Wang, J.; Bo, D. Adaptive fixed-time sensorless maximum power point tracking control scheme for DFIG wind energy conversion system. *Int. J. Electr. Power Energy Syst.* **2022**, *135*, 107424. [CrossRef]
7. Peng, B.; Zhang, F.; Liang, J.; Ding, L.; Liang, Z.; Wu, Q. Coordinated control strategy for the short-term frequency response of a DFIG-ES system based on wind speed zone classification and fuzzy logic control. *Int. J. Electr. Power Energy Syst.* **2019**, *107*, 363–378. [CrossRef]
8. Belmokhtar, K.; Doumbia, M.L.; Agbossou, K. Novel fuzzy logic based sensorless maximum power point tracking strategy for wind turbine systems driven DFIG (doubly-fed induction generator). *Energy* **2014**, *76*, 679–693. [CrossRef]
9. Sahri, Y.; Tamalouzt, S.; Lalouni Belaid, S.; Bacha, S.; Ullah, N.; Ahamdi, A.A.A.; Alzaed, A.N. Advanced Fuzzy 12 DTC Control of Doubly Fed Induction Generator for Optimal Power Extraction in Wind Turbine System under Random Wind Conditions. *Sustainability* **2021**, *13*, 11593. [CrossRef]
10. Khoete, S.; Manabe, Y.; Kurimoto, M.; Funabashi, T.; Kato, T. Robust H-infinity Control for DFIG to Enhance Transient Stability during Grid Faults. In Proceedings of the World Congress on Engineering and Computer Science, San Francisco, CA, USA, 19–21 October 2016.
11. Wei, J.; Li, C.; Wu, Q.; Zhou, B.; Xu, D.; Huang, S. MPC-based DC-link voltage control for enhanced high-voltage ride-through of offshore DFIG wind turbine. *Int. J. Electr. Power Energy Syst.* **2021**, *126*, 106591. [CrossRef]
12. Abdelrahem, M.; Hackl, C.; Kennel, R.; Rodriguez, J. Low Sensitivity Predictive Control for Doubly-Fed Induction Generators Based Wind Turbine Applications. *Sustainability* **2021**, *13*, 9150. [CrossRef]
13. Qin, S.J.; Badgwell, T.A. A survey of industrial model predictive control technology. *Control Eng. Pract.* **2003**, *11*, 733–764. [CrossRef]
14. Zhang, H.; Hao, J.; Wu, C.; Li, Y.; Sahab, A. A novel LMI-based robust adaptive model predictive control for DFIG-based wind energy conversion system. *Syst. Sci. Control Eng.* **2019**, *7*, 311–320. [CrossRef]
15. Darabian, M.; Jalilvand, A. Predictive control strategy to improve stability of DFIG-based wind generation connected to a large-scale power system. *Int. Trans. Electr. Energy Syst.* **2017**, *27*, e2300. [CrossRef]
16. Zhi, D.; Xu, L.; Williams, B.W. Model-based predictive direct power control of doubly fed induction generators. *IEEE Trans. Power Electron.* **2009**, *25*, 341–351.
17. Fezazi, O.; Ahmed, M. Predictive Control of Doubly Fed Induction Generator Used for Wind Energy. Ph.D. Thesis, Djillali Liabès university, Sidi Bel Abbès, Algeria, 2017.
18. Kou, P.; Liang, D.; Li, J.; Gao, L.; Ze, Q. Finite-control-set model predictive control for DFIG wind turbines. *IEEE Trans. Autom. Sci. Eng.* **2017**, *15*, 1004–1013. [CrossRef]
19. Nguyen, T.A.; Nguyen, H.T.; Phan, G.A.V.; Pham, V.; Vo, V.O.; Doan, P.T.; Pham, V.T.; Nguyen, K.A.; Rodriguez-Ayerbe, P.; Ngo, V.Q.B. An efficient model predictive control based on Lyapunov function for doubly fed induction generator fed by a T-type inverter. *Electr. Eng.* **2021**, *103*, 663–676. [CrossRef]
20. Ghodbane-Cherif, M.; Skander-Mustapha, S.; Slama-Belkhodja, I. An improved predictive control for parallel grid-connected doubly fed induction generator-based wind systems under unbalanced grid conditions. *Wind Eng.* **2019**, *43*, 377–391. [CrossRef]
21. Abad, G.; Rodriguez, M.A.; Poza, J. Two-level VSC based predictive direct torque control of the doubly fed induction machine with reduced torque and flux ripples at low constant switching frequency. *IEEE Trans. Power Electron.* **2008**, *23*, 1050–1061. [CrossRef]
22. Izanlo, A.; Kazemi, M.V.; Gholamian, A. A new method of predictive direct torque control for doubly fed induction generator under unbalanced grid voltage. *Rev. Roum. Sci. Techn.-Electrotechn. Energ.* **2018**, *63*, 332–337.
23. Kennel, R.; Linder, A.; Linke, M. Generalized predictive control (GPC)-ready for use in drive applications? In Proceedings of the 2001 IEEE 32nd Annual Power Electronics Specialists Conference (IEEE Cat. No. 01CH37230), Vancouver, BC, Canada, 17–21 June 2001; Volume 4, pp. 1839–1844.
24. Solís-Chaves, J.S.; Rodrigues, L.L.; Rocha-Osorio, C.; Sguarezi Filho, A.J. A long-range generalized predictive control algorithm for a DFIG based wind energy system. *IEEE/CAA J. Autom. Sin.* **2019**, *6*, 1209–1219. [CrossRef]
25. Rodrigues, L.L.; Vilcanqui, O.A.; Guerero, J.M.; Sguarezi Filho, A.J. Generalized Predictive Control applied to the DFIG power control using state-space model and voltage constraints. *Electr. Power Syst. Res.* **2020**, *182*, 106227. [CrossRef]
26. Zhang, J.; Wang, H.; Hou, G.; Zhang, J. Generalized predictive control for wind turbine systems. In Proceedings of the 2010 5th IEEE Conference on Industrial Electronics and Applications, Taichung, Taiwan, 15–17 June 2010; pp. 679–683.

27. Roy, J.S. TNC: A Non Linear Optimization Package. 2004. Available online: http://js2007.free.fr/code/index.html (accessed on 24 May 2022).
28. Akhmatov, V. Variable-speed wind turbines with doubly-fed induction generators: Part i: Modelling in dynamic simulation tools. *Wind Eng.* **2002**, *26*, 85–108. [CrossRef]
29. Song, Y.; Dhinakaran, B.; Bao, X. Variable speed control of wind turbines using nonlinear and adaptive algorithms. *J. Wind Eng. Ind. Aerodyn.* **2000**, *85*, 293–308. [CrossRef]
30. Rakovic, S.V. Robust Model-Predictive Control. 2015. Available online: https://www.researchgate.net/profile/Sasa-V-Rakovic/publication/291956851_Robust_Model_Predictive_Control/links/5aa2cf79aca272d448b5a493/Robust-Model-Predictive-Control.pdf (accessed on 16 January 2018).
31. Camacho, E.F.; Alba, C.B. *Model Predictive Control*; Springer Science & Business Media: Cham, Switzerland, 2013.
32. Gomma, H.W.; Owens, D.H. Stability analysis for generalized predictive control (GPC) and time varying weighting generalized predictive control (TGPC). In Proceedings of the 2004 IEEE International Conference on Control Applications, Taipei, Taiwan, 2–4 September 2004; Volume 2, pp. 1662–1667.
33. Mohan, N. *Advanced Electric Drives: Analysis, Control, and Modeling Using MATLAB/Simulink*; John Wiley & Sons: Hoboken, NJ, USA, 2014.